

1 **Version: Accepted manuscript version**

2 Jadreško, D., and M. Zelić. 2015. "Square-Wave Voltammetry of Electroinactive
3 Surfactants." *Electroanalysis* 27 (7): 1669–75. doi:10.1002/elan.201400692.

4

5

6

7 **Square-wave voltammetry of electroinactive surfactants**

8 Dijana Jadreško*, Marina Zelić

9 Division for Marine and Environmental Research, Ruder Bošković Institute, P.O. Box 180,
10 HR-10002 Zagreb, Croatia

11 *e-mail address: djadresko@irb.hr

12

13 Abstract

14 Under the influence of previously published and some new theoretical results, potential-
15 dependent adsorption and desorption of model electroinactive surfactants Triton X-100 (T-
16 X-100 or polyethylene glycol p-(1,1,3,3-tetramethylbutyl)-phenyl ether) and sodium
17 dodecyl sulfate (SDS) on the static mercury drop electrode (SMDE) were studied by
18 square-wave voltammetry (SWV). Although (according to the theory) the resulting current
19 – potential curve should consist of two highly separated peaks, only desorption signal
20 could be seen on each experimentally obtained voltammogram, most probably because of
21 the limitations concerning the available potential range. Different properties of the
22 recorded peak are in good agreement with the theory indicating that square-wave
23 voltammetry could be treated as a potential tool for tensammetric studies of
24 electroinactive surface active substances.

25

26 Keywords

27 Adsorption/desorption, electroinactive substances, square-wave voltammetry,
28 tensammetry.

29

30 **1. Introduction**

1 Electroanalytical studies of adsorption processes at electrode surfaces have been in focus
2 for many years. The current response depends on whether the electro- active or inactive
3 substances adsorb on the working electrode [1-12]. Modern electrochemical instrumentation
4 enables independent measurements of the faradaic and capacitive components of the current
5 that flows across the electrode-electrolyte interface. Therefore, alternating current
6 voltammetry is the most commonly used technique for the study of surface processes without
7 electron transfer [1,12-16]. Electroanalysis of electroinactive surfactants is based on recording
8 of their influence upon the electrode double layer structure. During adsorption of a redox
9 inactive substance, the electrical double layer capacitance and thus the capacitive current
10 decrease [13]. The measurement of *ac* capacitive current as a function of electrode potential is
11 called tensammetry [17,18] but the same term is used when other voltammetric techniques are
12 applied for the similar purpose. The potential region of low-capacity values is limited on both
13 high-potential and low-potential sides by adsorption-desorption peaks, which reflect sharp
14 changes in the surface charge within a narrow potential range [1,19].

15 On the other hand, square-wave voltammetry is generally considered as being insensitive
16 to capacitive current [20], i.e. one of the main advantages of SWV is its ability to effectively
17 discriminate against charging current [21]. More precisely, SW voltammetry is a powerful
18 electrochemical technique for kinetic and mechanistic studies as well as analytical
19 examinations of faradaic processes [20,22-25]. Although some attempts of its application in
20 the analysis of electroinactive surfactants were described [26], systematic studies of such a
21 “new” method are not known. In the previous article from our laboratory [27] a basic theory
22 of square wave voltammetry of surface-active, electroinactive compounds was developed. It
23 was shown that tensammetric/desorption peak originates from the difference in surface
24 coverage during the forward and backward series of pulses of SWV signal.

25 In this article, experimentally obtained SW current - potential curves of model
26 electroinactive surfactants Triton X-100 and sodium dodecyl sulfate will be presented and
27 treated in the light of previously published [27] and some new theoretical results.

28

29 **2. Experimental**

30 All chemicals used in the experiments were of the best grade commercially available
31 (Sigma-Aldrich) and were used without further purification. Model solutions of surface active
32 substances (Triton X-100 and SDS) were prepared by diluting the same concentrated solution

1 (i.e. 5.62 g/L and 1×10^{-2} mol/L respectively). All solutions were prepared with water purified
2 in a Milipore Mili-Q system.

3 All voltammograms were recorded using a static mercury drop electrode (SMDE 663 VA
4 Stand from Metrohm). A platinum rod served as a counter electrode whereas all potentials
5 were given with respect to Ag/AgCl (3 mol/L KCl) with 3 mol/L NaCl in the electrolyte
6 bridge (to prevent formation of sparingly soluble KClO_4 in the frit).

7 The electrode system was attached through the corresponding IME (Interface for Mercury
8 Electrode) module to the „PGSTAT 101“ instrument (from Eco Chemie, Utrecht), controlled
9 by the electrochemical software “NOVA 1.5”.

10 Before starting each new set of measurements, the solution in the electrolytic cell was
11 deaerated with high purity (99.999%) nitrogen for 15 min. The room temperature was
12 maintained at 25 ± 1 °C. All measurements were carried out on “small size” mercury drops (S
13 $= 0.265 \text{ mm}^2$) using 1 mol/L NaClO_4 as supporting electrolyte.

14

15 **3. The model**

16 A simple potential dependent electrode reaction was assumed:



18 According to the previous results [27] the normalized SWV response is defined by
19 expression:

20

$$21 \quad i \cdot (SC_{\theta=0} f)^{-1} = \Delta E \cdot (C_{\theta=1}/C_{\theta=0} - 1) \cdot 50 \cdot (\theta_{m-1} - \theta_m) \quad (2)$$

22 in which $\Delta E = E - E_{\text{pzc}}$ whereas other symbols have their usual meanings, given in
23 Table 1. The constant 50 on the right side of equation 2 reflects the applied time
24 increment ($\Delta t = (50 \cdot f)^{-1}$). Other details of the simulation procedure are given in reference
25 [27].

26 The model was developed to simulate the experiments with static mercury drop
27 electrode, assuming that 1) adsorption of the studied surfactant can be described by
28 Langmuir or Frumkin isotherm (with attractive interactions) and 2) potential of zero
29 charge is not affected by addition of surface active substances to the electrolyte solution.

30 From the practical point of view it is important that the normalized SW current
31 depends on four parameters which are related to the a) bulk concentration of the reactant
32 ($y = c^* D^{1/2}/(\Gamma_{\text{max}} \cdot f^{1/2})$), b) maximum adsorption constant ($b_0 = \beta_0 \cdot \Gamma_{\text{max}} \cdot f^{1/2} D^{-1/2}$), c)

1 capacity of a double layer on the free electrode surface ($k_c = C_{\theta=0} \cdot (1 -$
2 $(C_{\theta=1}/C_{\theta=0})) / (2RTT_{\max})$) and d) ratio of capacities of totally covered and free electrode
3 surfaces ($C_{\theta=1}/C_{\theta=0}$). In addition, SWV response depends on the Frumkin coefficient
4 and the relationship between the potential of zero charge and the surface coverage as
5 well.

6

7 **4. Results and discussion**

8 **4.1. Theory**

9 According to the published theoretical results [27], a square-wave voltammogram of
10 an electroinactive surfactant is generally characterized by a well defined desorption peak,
11 assuming that scanning in the negative direction starts near the potential of zero charge
12 whereas the whole process could be described by equation 1. When a (much) more
13 positive starting potential is applied instead, the response of the type given in Fig. 1A is to
14 be expected. It consists of two highly separated peaks with a zero current range between
15 them. As pointed out elsewhere [27], tensammetric peaks in SWV reflect the difference in
16 surface coverage during forward and backward series of pulses. From Fig. 1B, which
17 gives surface coverage in dependence on the electrode potential, it follows that the more
18 positive peak results from the gradual adsorption of the studied surfactant whereas the
19 more negative peak (at $E \ll E_{pzc}$) is a consequence of desorption process. In the range
20 between them, the maximum coverage of the electrode surface ($\theta = 1$) is achieved.
21 Taking into account that simple, potential dependent adsorption is assumed, the values of
22 the initial and final potential from Fig. 1A could be interchanged. Such a scanning in the
23 positive direction should give the same pair of peaks as before but oriented in the opposite
24 direction (Fig. 1C) as a result of the difference in surface coverage at negative and
25 positive pulses (Fig. 1D). In such an experiment the more positive signal is expected to
26 be higher than the more negative one whereas in Fig. 1A the opposite is true. At higher
27 values of the concentration parameter, the difference between two peaks gradually disappears.

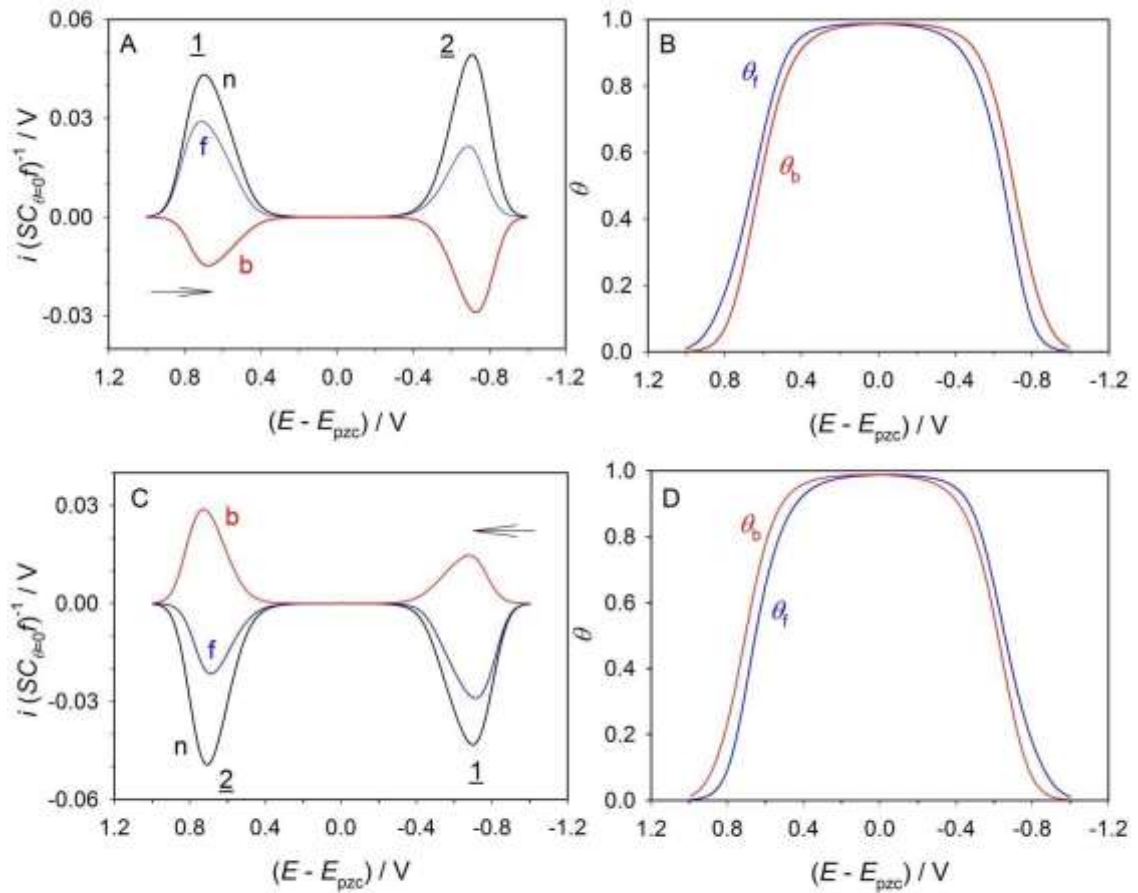


Figure 1

1
2 Fig. 1. (A) Normalized SW net voltammogram (n) along with its forward (f) and backward (b)
3 components. (B) Dependence of the electrode surface coverage on the electrode potential. (C)
4 and (D) The same as (A) and (B) but for the opposite scan direction (indicated by an arrow).
5 Conditions: $E_{st} = (-) 1 \text{ V vs. } E_{pzc}$, $E_s = 5 \text{ mV}$, $E_{sw} = 50 \text{ mV}$, $y = 0.3$, $k_c = 10 \text{ V}^{-2}$, $b_0 = 333$,
6 $C_{\theta=1}/C_{\theta=0} = 0.5$, $a = 0$ and $E_{pzc,\theta=1} = E_{pzc,\theta=0}$.

7

8 4.2. Model experiments

- 9 In order to test the theoretical results, experimental studies were performed with Triton X-
10 100 and sodium dodecyl sulfate (SDS), as “representatives” of nonionic and negatively
11 charged surface active substances. In Fig. 2, desorption peaks of Triton X-100 along with
12 components of some net currents are given for the concentration range 0.50 - 9.80 mg/L.
13 The concentrations are given in mg/L because molecular weight of Triton X-100 is not well
14 defined [28] (as a result of the fact that in the formula $C_{14}H_{22}O(C_2H_4O)_n$, $n = 9 - 10$). If the

1 approximate value of 625 is applied for calculations, it follows that the measurements were
2 performed in the range 0.800 – 15.68 $\mu\text{mol/L}$.

3

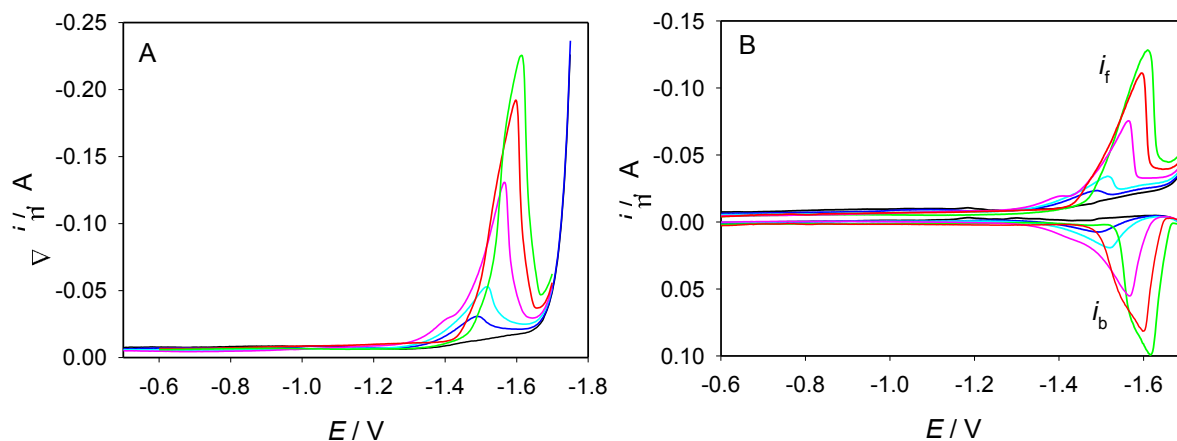


Figure 2

4

5 Fig. 2. (A) Square-wave net voltammograms of T-X-100. (B) Their forward (i_f) and
6 backward (i_b) components. Surfactant concentrations: 0, 0.50, 1.00, 2.98, 5.93 and 9.80
7 mg/L in 1 mol/L NaClO_4 . $E_{st} = -0.5$ V, $E_{sw} = 50$ mV, $E_s = 2$ mV, $f = 50$ s $^{-1}$.

8

9 By inspection of Fig. 2, it could be noticed that adsorption peak does not appear,
10 irrespective of the surfactant concentration, when scanning in the negative direction starts at -
11 0.5 V. Shifting of the starting potential to the most positive values (accessible in experiments
12 with SMDE), even after elimination of chloride ions from the electrolyte bridge (i.e. their
13 substitution with nitrates) does not change the properties of the electrode response, i.e.
14 adsorption peak stays “invisible”. All desorption signals are of the similar shape, their
15 backward components are well defined, whereas peak potential becomes more negative as the
16 analyte concentration increases ($dE_p/d \log c = -100$ mV/d.u.).

17 When the similar set of voltammograms of SDS is recorded (Fig. 3), final conclusions are
18 the same as for Triton X-100 as long as analyte concentration is kept within the range 5
19 $\mu\text{mol/L}$ – 0.1 mmol/L. At (significantly) higher levels of the dissolved surfactant, the signal
20 becomes extremely sharp and split in two close peaks. The formal origin of such splitting
21 could be found in the fact that components of the net current are shifted, one with respect to
22 the other (Fig. 3B).

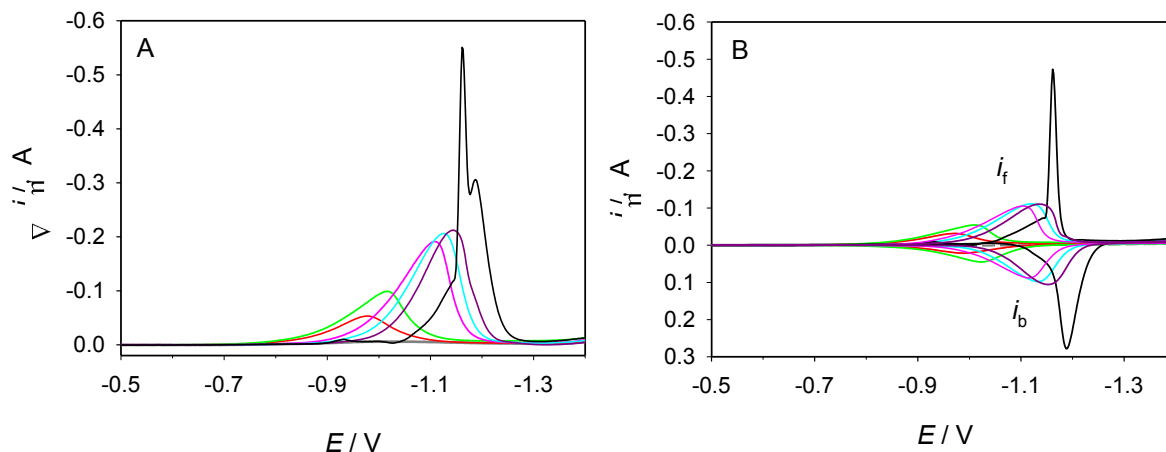


Figure 3

1
 2 Fig. 3. (A) Square-wave net voltammograms of SDS. (B) Their forward (i_f) and backward
 3 (i_b) components. Surfactant concentrations: 0, 5.0, 10.0, 49.8, 69.5, 99.0 and 291.0
 4 $\mu\text{mol/L}$ in 1 mol/L NaClO_4 . $E_{st} = -0.5 \text{ V}$, $E_{sw} = 50 \text{ mV}$, $E_s = 2 \text{ mV}$, $f = 50 \text{ s}^{-1}$.

5
 6 Similar effects, i.e. the dependence of *ac* experimental results on the reactant
 7 concentration were previously observed by other authors [29] and ascribed to different types
 8 of molecular associations. In order to avoid the mentioned “complications”, all other
 9 measurements were performed at $c(\text{SDS}) \leq 2 \times 10^{-5} \text{ mol/L}$. It is possible that the described and
 10 some other changes in the peak properties could be useful analytical tools for recognition of
 11 the systems, in which electrode reaction cannot be described as a simple, potential dependent
 12 adsorption of an electroinactive surfactant. For such an application of SWV, additional
 13 theoretical results and experimental measurements are needed.

14 Theoretical dependence of the normalized SWV peak current on the concentration
 15 parameter y is given in Fig. 4. It was calculated for $k_c = 10 \text{ V}^{-2}$, $C_{\theta=1}/C_{\theta=0} = 0.5$ [27] and $b_0 =$
 16 236, corresponding to $\Gamma_{\text{max}} = 10^{-9} \text{ mol/cm}^2$, $D = 9 \times 10^{-6} \text{ cm}^2/\text{s}$, $\beta_0 = 10^8 \text{ cm}^3/\text{mol}$ [27] and a
 17 value of SW frequency $f = 50 \text{ Hz}$. Experimentally obtained current - concentration plot should
 18 be of the same type, when measurements (under otherwise identical conditions) are performed
 19 at increasing concentration of the studied surfactant. For Triton X-100, the agreement of
 20 experimental results with theory is good. The only (formal) difference could be found in the
 21 sign of current because its positive value was (arbitrarily) assumed during theoretical
 22 treatment of the whole problem, whereas measured value was always negative. The net peak
 23 current increases (linearly) with increasing surfactant concentration until the electrode surface
 24 saturation is achieved. Thus, the quasi-linear range for $\chi(\text{Triton X-100}) \leq 3 \text{ mg/L}$ (regression

1 line: $-\Delta i_p / A = (0.0372 \cdot \gamma / \text{mg L}^{-1} - 0.0034) \times 10^{-6}$, $R^2 = 0.994$) could be suitable for
 2 determinations of T-X-100 with detection limit of 0.1 mg/L. The detection limit can be
 3 lowered by introduction of the accumulation step prior the potential scanning in SWV
 4 experiment. In addition, for practical purposes, such as measurement of an unknown
 5 concentration, it is useful to find conditions under which current-concentration plot could be
 6 described as a straight line with (virtually) zero intercept. This can be achieved by proper
 7 choice of square-wave amplitude.

8

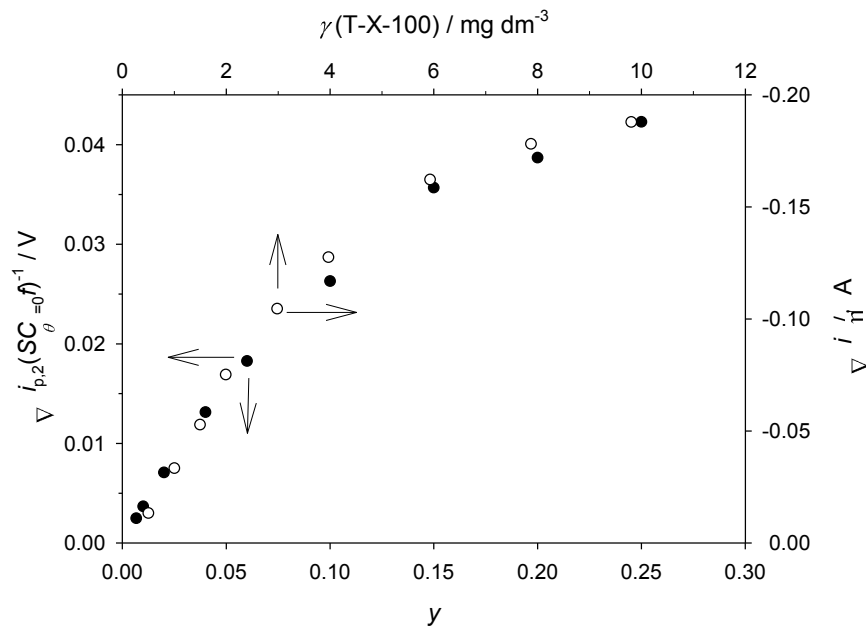


Figure 4

9

10 Fig. 4. (●) Theoretical influence of dimensionless concentration parameter y on the
 11 normalized desorption net peak current for $E_{st} = -0.2 \text{ V}$ vs. E_{pzc} , $E_{sw} = 50 \text{ mV}$, $k_c = 10 \text{ V}^{-2}$,
 12 $C_{\theta=1}/C_{\theta=0} = 0.5$, $a = 0$, $E_{pzc,\theta=1} = E_{pzc,\theta=0}$, $b_0 = 236$ and $E_s = 2 \text{ mV}$. (○) Dependence of the real
 13 desorption net peak current on concentration of T-X-100 (in 1 mol/L NaClO_4) for conditions
 14 given in description of Fig. 2.

15

16 The absence of adsorption peaks on all experimentally obtained tensammetric SWV
 17 curves is not fully unexpected. According to model calculations, for conditions given in
 18 description of Fig. 1, separation of the two signals should be highly pronounced and
 19 additionally dependent on the value of Frumkin coefficient (Fig. 5). In other words, one peak
 20 could be shifted with respect to the other for 1.4 – 1.5 V (or even more) under real conditions.
 21 At the same time the half-peak width could be highly reduced in comparison with the value
 22 for $a = 0$.

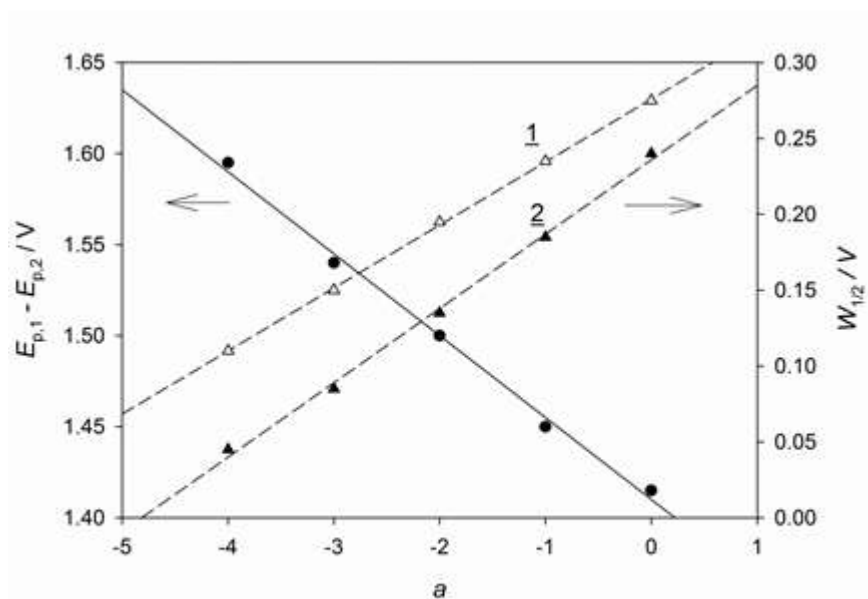


Figure 5

1
 2 Fig. 5. (●) Theoretical dependence of potential difference between adsorption (1) and
 3 desorption (2) peaks of SWV signal and (△, ▲) their half-peak widths on Frumkin coefficient.
 4 Other parameters are given in description of Fig. 1.

5
 6 Although tensammetric measurements are generally performed on mercury (because
 7 its clean surface can be obtained again and again without difficulties), the additional
 8 application of some other electrode material, on which scanning in a wider potential range
 9 (that includes more positive values than in the present case) is possible, seems promising for
 10 some purposes. The point is that only in such a way the electrode response from Fig. 1A
 11 could be obtained in real experiments. When only desorption peak appears, it could be a
 12 problem to make difference between it and the signal that reflects reduction from the adsorbed
 13 state, because current – frequency linearity (Fig. 6) and current – concentration plots of the
 14 same type (Fig. 4) arise from both electrode processes.

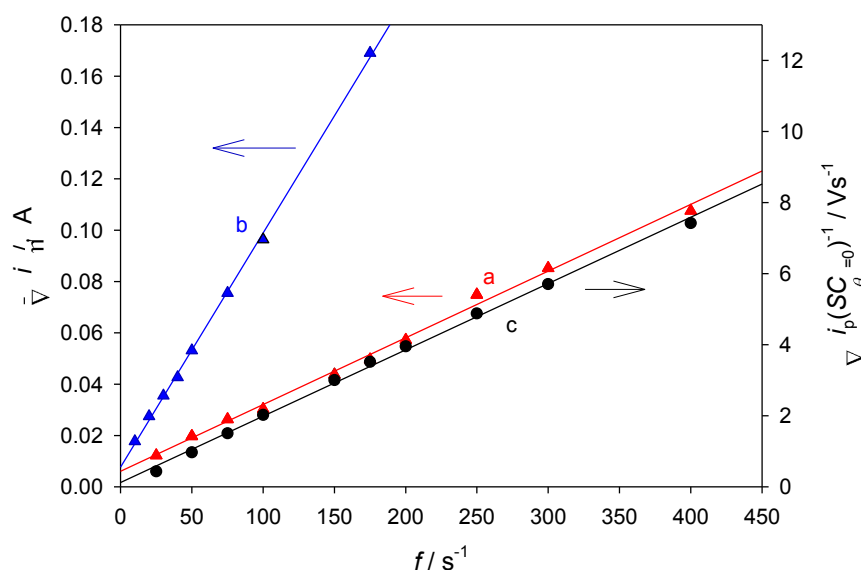


Figure 6

1
 2 Fig. 6. Dependence of the experimentally obtained (a, b) and normalized theoretical (c)
 3 desorption SWV net peak currents on SW frequency. Conditions: a) 1 mg/L T-X-100 ($E_{sw} =$
 4 20 mV) and b) 5×10^{-6} mol/L SDS ($E_{sw} = 50$ mV) in 1 mol/L NaClO₄; $E_s = 2$ mV. c) $D = 9 \times$
 5 10^{-6} cm²s⁻¹, $c^* = 10^{-3}$ mol/L, $\Gamma_{max} = 10^{-9}$ mol/cm², $\beta_0 = 10^8$ cm³/mol, $a = 0$, $E_{pzc,\theta=1} = E_{pzc,\theta=0}$, E_s
 6 = 2 mV and $E_{sw} = 20$ mV.

7
 8 Therefore only the full tensammetric curve with two well defined and highly separated
 9 peaks becomes the best qualitative indicator of the electroinactive surfactant and its surface
 10 reactions. It is because in a Faradaic process, complicated by reactant adsorption, broadening
 11 of the signal or appearance of two, poorly separated peaks could usually be noticed at
 12 relatively high reactant concentrations [9] whereas only in the case of tensammetric signals,
 13 i.e. adsorption/desorption of surface active but electroinactive solutes, two well defined but
 14 highly separated signals are to be expected.

15 From Figs. 1A and 1C, it follows that cyclic square-wave voltammetry could also be
 16 applicable in experimental studies of electroinactive surfactants. The mentioned technique
 17 was recently developed and applied for characterization of kinetically controlled faradaic
 18 processes [30,31]. Its potential “strength” in tensammetry is not quite clear but it is worth
 19 further examination. An example of the resulting current – potential curves for different
 20 concentrations of anionic surfactant SDS is given in Fig.7.

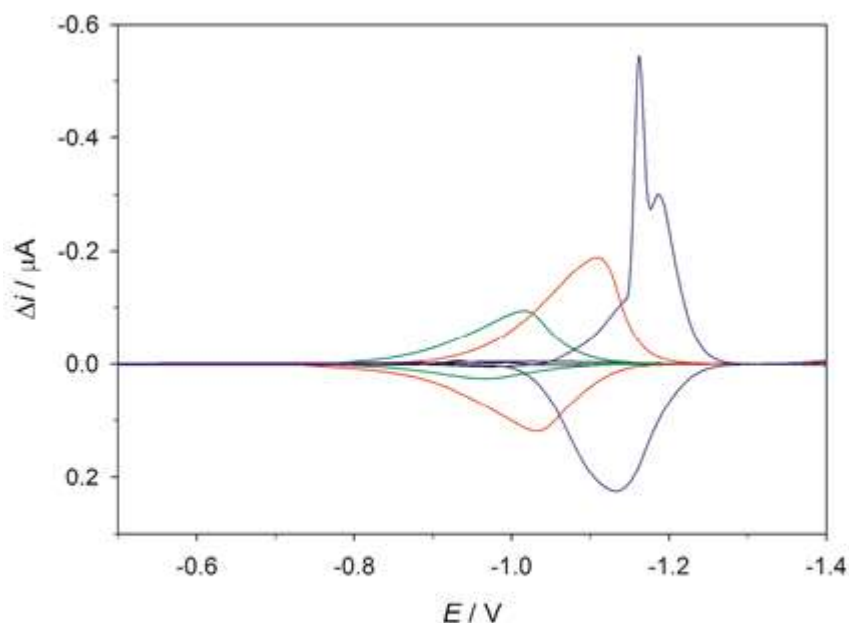


Figure 7

Fig. 7. Cyclic square-wave voltammograms of SDS for conditions given in description of Fig.2. Surfactant concentrations: 0 (black), 10.0 (green), 49.8 (red) and 291.0 $\mu\text{mol/L}$ in 1 mol/L NaClO_4 .

5. Conclusions

From the theoretical and experimental results, it follows that a pronounced electrode response is to be expected when square wave voltammogram of an electroinactive surfactant is recorded. This is important for at least three reasons because it indicates that: a) SWV signal obtained during analysis of an unknown sample does not always reflect a redox reaction b) SWV is not so insensitive to capacitive currents as usually stated and c) the technique is a potential tool for different studies of adsorption/desorption processes and trace analysis of surface active substances. The latter is possible because the signal could be highly increased if accumulation step is included.

Although the whole current – potential curve should consist of two highly separated peaks which reflect adsorption and desorption reactions, i.e. a pronounced change of surface coverage within a narrow potential range in each case, real measurements on SMDE give only a desorption signal. Most probably, the problem arises from the fact that really positive potentials are not available in experiments with a mercury electrode. For many practical

1 purposes, however, the presence of only one peak is sufficient especially because of the fact
2 that its properties are in good agreement with the theory.

3 Taking into account that measurements of electroinactive surfactants is usually performed
4 by *ac* voltammetry it is of prime importance to compare such results with those that arise
5 from the application of square wave voltammetry, i.e. to find if SWV could be applied in
6 addition to *ac* voltammetry or even instead of it.

7

8 **Acknowledgements**

9 The authors would like to thank to Dr. Sc. Milivoj Lovrić for helpful discussion and
10 advices.

11

1 6. References

- 2 [1] A. N. Frumkin, B. B. Damaskin in *Modern aspects of electrochemistry no. 3* (Eds.:
3 J. O. M. Bockris, B. E. Conway), Butterworths, London, **1964**, pp. 149-223.
- 4 [2] H. P. van Leeuwen, M. Sluyters-Rehbach, K. Holub, *J. Electroanal. Chem.* **1982**,
5 *135*, 13-24.
- 6 [3] M. Lovrić, Š. Komorsky-Lovrić, *J. Electroanal. Chem.* **1988**, *248*, 239-253.
- 7 [4] M. Seralathan, A. Ribes, J. O'Dea, J. Osteryoung, *J. Electroanal. Chem.* **1991**,
8 *306*, 195-211.
- 9 [5] G. Wittstock, H. Emons, *Electrochim. Acta* **1992**, *37*, 2395-2401.
- 10 [6] H. P. van Leeuwen, J. Buffle, M. Lovrić, *Pure Appl. Chem.* **1992**, *64*, 1015-1028.
- 11 [7] Š. Komorsky-Lovrić, M. Lovrić, M. Branica, *Electroanalysis* **1995**, *7*, 652-655.
- 12 [8] Š. Komorsky-Lovrić, *Electroanalysis* **2000**, *12*, 599-604.
- 13 [9] M. Lovrić, *Electroanalysis* **2002**, *14*, 405-414.
- 14 [10] B. Gašparović, D. Risović, B. Čosović, *Electrochim. Acta* **2004**, *49*, 3383-3396.
- 15 [11] M. Lovrić, M. Zelić, *J. Electroanal. Chem.* **2008**, *624*, 174-178.
- 16 [12] B. Čosović, Z. Kozarac, S. Frka, V. Vojvodić, *Electroanalysis* **2010**, *22*, 1994-2000.
- 17 [13] B. B. Damaskin, *Electrochim. Acta* **1964**, *9*, 231-240.
- 18 [14] D. R. Canterford, *J. Electroanal. Chem.* **1981**, *118*, 395-403.
- 19 [15] Z. Lukaszewski, H. Batycka, W. Zembrzuski, *Anal. Chim. Acta* **1985**, *175*, 55-67.
- 20 [16] B. Čosović in *Aquatic chemical kinetic* (Ed.: W. Stumm), Wiley, New York, **1990**,
21 pp. 291-309.
- 22 [17] B. Breyer, H.H. Bauer, *Alternating current polarography and tensametry*, Wiley-
23 Interscience, New York, **1963**.
- 24 [18] Z. Lukaszewski, *Electroanalysis* **1993**, *5*, 375-384.
- 25 [19] H. Jehring, *Elektrosorptionanalyse mit der Wechselstrom Polarographie*, Akademie
26 Verlag, Berlin, **1974**.
- 27 [20] V. Mirčeski, Š. Komorsky-Lovrić, M. Lovrić, *Square-wave voltammetry*, Springer,
28 Berlin, **2007**.
- 29 [21] J. G. Osteryoung, R. A. Osteryoung, *Anal. Chem.* **1985**, *57*, 101A-110A.
- 30 [22] J. Osteryoung, J. J. O'Dea in *Electroanalytical chemistry Vol. 14* (Ed.: A. J. Bard),
31 Marcel Dekker, New York, **1986**, pp. 209-303.
- 32 [23] J. J. O'Dea, J. Osteryoung, R. A. Osteryoung, *Anal. Chem.* **1981**, *53*, 695-701.
- 33 [24] M. J. Nuwer, J. J. O'Dea, J. Osteryoung, *Anal. Chim. Acta* **1991**, *251*, 13-25.

- 1 [25] N. Fatouros, D. Krulic, *J. Electroanal. Chem.* **1998**, *443*, 262-265.
- 2 [26] A. Safavi, N. Maleki, H. R. Shahbaazi, *Anal. Chim. Acta* **2003**, *494*, 225-233.
- 3 [27] D. Jadreško, M. Lovrić, *Electrochim. Acta* **2008**, *53*, 8045-8050.
- 4 [28]<https://www.sigmaaldrich.com/content/dam/sigma->
- 5 [aldrich/docs/Sigma/Product_Information_Sheet/1/t8532pis.pdf](https://www.sigmaaldrich.com/content/dam/sigma-aldrich/docs/Sigma/Product_Information_Sheet/1/t8532pis.pdf)
- 6 [29] B. Gašparović, D. Risović, B. Ćosović, A. Nelson, *Electrochim. Acta*
- 7 **2007**, *52*, 2527- 2534, and references therein.
- 8 [30] D. Jadreško, M. Zelić, *J. Electroanal. Chem.* **2013**, *707*, 20-30.
- 9 [31] D. Jadreško, M. Zelić, *J. Electroanal. Chem.* **2014**, *714-715*, 30-37.

10

Table 1. List of symbols

a	Frumkin coefficient
b_0	dimensionless adsorption constant
c	concentration of the reactant
c^*	bulk concentration of the reactant
$C_{\theta=0}$	capacity of free electrode surface
$C_{\theta=1}$	capacity of totally covered electrode surface
D	diffusion coefficient
E	electrode potential
E_{pzc}	potential of zero charge
$E_{pzc,\theta=0}$	potential of zero charge of free electrode surface
$E_{pzc,\theta=1}$	potential of zero charge of totally covered electrode surface
E_s	SW potential step
E_{st}	starting potential
E_{sw}	SW amplitude
ΔE	difference between electrode potential and potential of zero charge
f	SW frequency
i	capacitive current
$i(S C_{\theta=0} f)^{-1}$	normalized SWV response
Δi	net current
i_f	forward component of net current in SWV
i_b	backward component of net current in SWV
Δi_p	net peak current
k_c	capacity parameter
R	gas constant
S	electrode surface area
T	temperature
$W_{1/2}$	half-peak width
y	dimensionless concentration parameter
β_0	adsorption constant at $E = E_{pzc}$
γ	mass concentration
Γ	surface concentration of the adsorbed reactant
Γ_{max}	maximum surface concentration of the adsorbed reactant
$\theta = \Gamma / \Gamma_{max}$	electrode surface coverage

1 **Figures Caption**

2 **Fig. 1.** (A) Normalized SW net voltammogram (n) along with its forward (f) and backward
3 (b) components. (B) Dependence of the electrode surface coverage on the electrode potential.
4 (C) and (D) The same as (A) and (B) but for the opposite scan direction (indicated by an
5 arrow). Conditions: $E_{st} = (-) 1 \text{ V}$ vs. E_{pzc} , $E_s = 5 \text{ mV}$, $E_{sw} = 50 \text{ mV}$, $y = 0.3$, $k_c = 10 \text{ V}^{-2}$, $b_0 =$
6 333 , $C_{\theta=1}/C_{\theta=0} = 0.5$, $a = 0$ and $E_{pzc,\theta=1} = E_{pzc,\theta=0}$.

7 **Fig. 2.** (A) Square-wave net voltammograms of T-X-100. (B) Their forward (i_f) and backward
8 (i_b) components. Surfactant concentrations: 0, 0.50, 1.00, 2.98, 5.93 and 9.80 mg/L in 1 mol/L
9 NaClO_4 . $E_{st} = -0.5 \text{ V}$, $E_{sw} = 50 \text{ mV}$, $E_s = 2 \text{ mV}$, $f = 50 \text{ s}^{-1}$.

10 **Fig. 3.** (A) Square-wave net voltammograms of SDS. (B) Their forward (i_f) and backward (i_b)
11 components. Surfactant concentrations: 0, 5.0, 10.0, 49.8, 69.5, 99.0 and 291.0 $\mu\text{mol/L}$ in 1
12 mol/L NaClO_4 . $E_{st} = -0.5 \text{ V}$, $E_{sw} = 50 \text{ mV}$, $E_s = 2 \text{ mV}$, $f = 50 \text{ s}^{-1}$.

13 **Fig. 4.** (●) Theoretical influence of dimensionless concentration parameter y on the
14 normalized desorption net peak current for $E_{st} = -0.2 \text{ V}$ vs. E_{pzc} , $E_{sw} = 50 \text{ mV}$, $k_c = 10 \text{ V}^{-2}$,
15 $C_{\theta=1}/C_{\theta=0} = 0.5$, $a = 0$, $E_{pzc,\theta=1} = E_{pzc,\theta=0}$, $b_0 = 236$ and $E_s = 2 \text{ mV}$. (○) Dependence of real
16 desorption net peak current on concentration of T-X-100 (in 1 mol/L NaClO_4) for conditions
17 given in description of Fig. 2.

18 **Fig. 5.** (●) Theoretical dependence of potential difference between adsorption (1) and
19 desorption (2) peaks of SWV signal and (Δ , \blacktriangle) their half-peak widths on Frumkin
20 coefficient. Other parameters are given in description of Fig. 1.

21 **Fig. 6.** Dependence of the experimentally obtained (a, b) and normalized theoretical (c)
22 desorption SWV net peak currents on SW frequency. Conditions: a) 1 mg/L T-X-100 ($E_{sw} =$
23 20 mV) and b) $5 \times 10^{-6} \text{ mol/L}$ SDS ($E_{sw} = 50 \text{ mV}$) in 1 mol/L NaClO_4 ; $E_s = 2 \text{ mV}$. c) $D = 9 \times$
24 $10^{-6} \text{ cm}^2 \text{ s}^{-1}$, $c^* = 10^{-3} \text{ mol/L}$, $\Gamma_{\max} = 10^{-9} \text{ mol/cm}^2$, $\beta_0 = 10^8 \text{ cm}^3/\text{mol}$, $a = 0$, $E_{pzc,\theta=1} = E_{pzc,\theta=0}$, E_s
25 $= 2 \text{ mV}$ and $E_{sw} = 20 \text{ mV}$.

26 **Fig. 7.** Cyclic square-wave voltammograms of SDS for conditions given in description of
27 Fig.2. Surfactant concentrations: 0 (black), 10.0 (green), 49.8 (red) and 291.0 (blue) $\mu\text{mol/L}$
28 in 1 mol/L NaClO_4 .

29

30

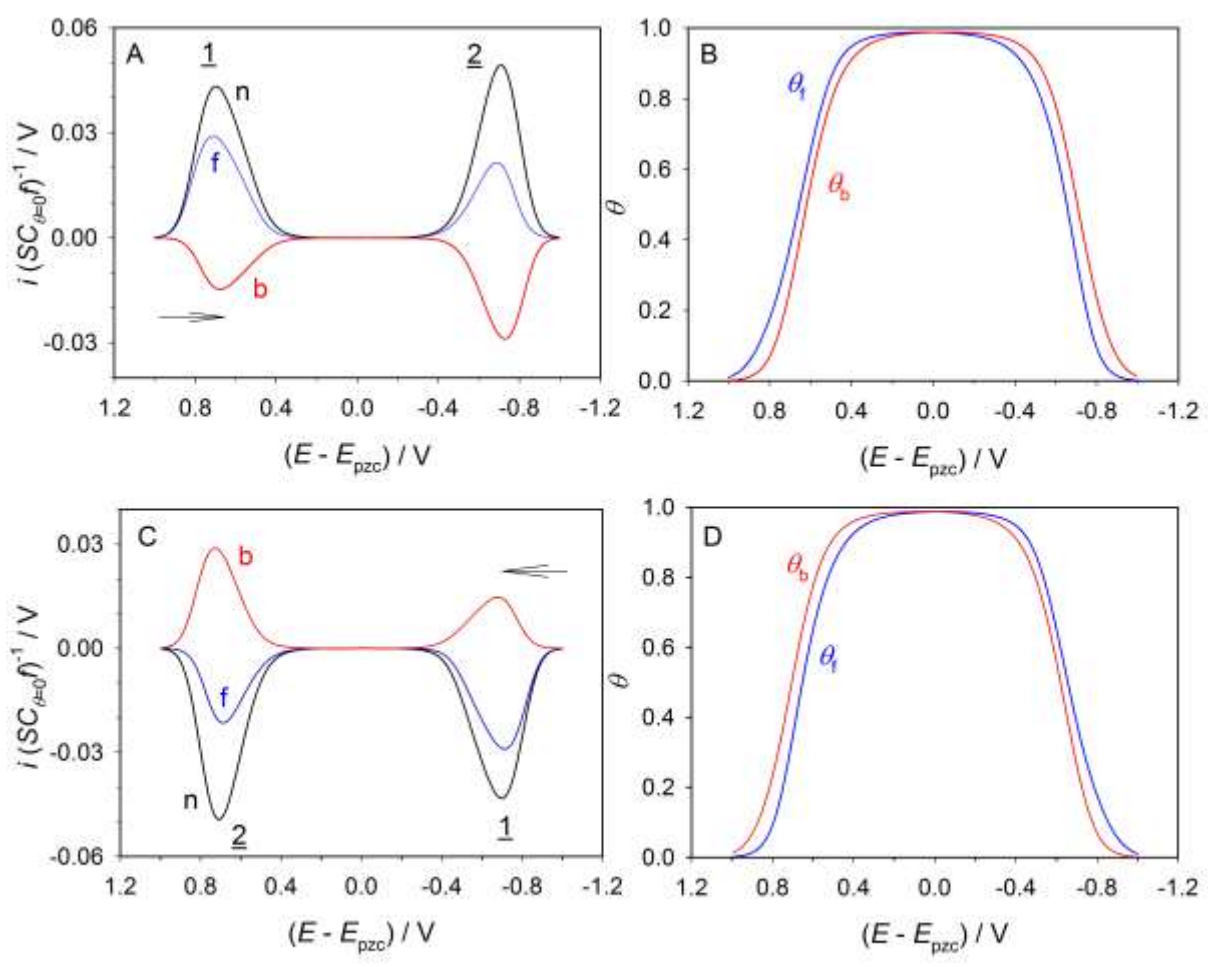


Figure 1

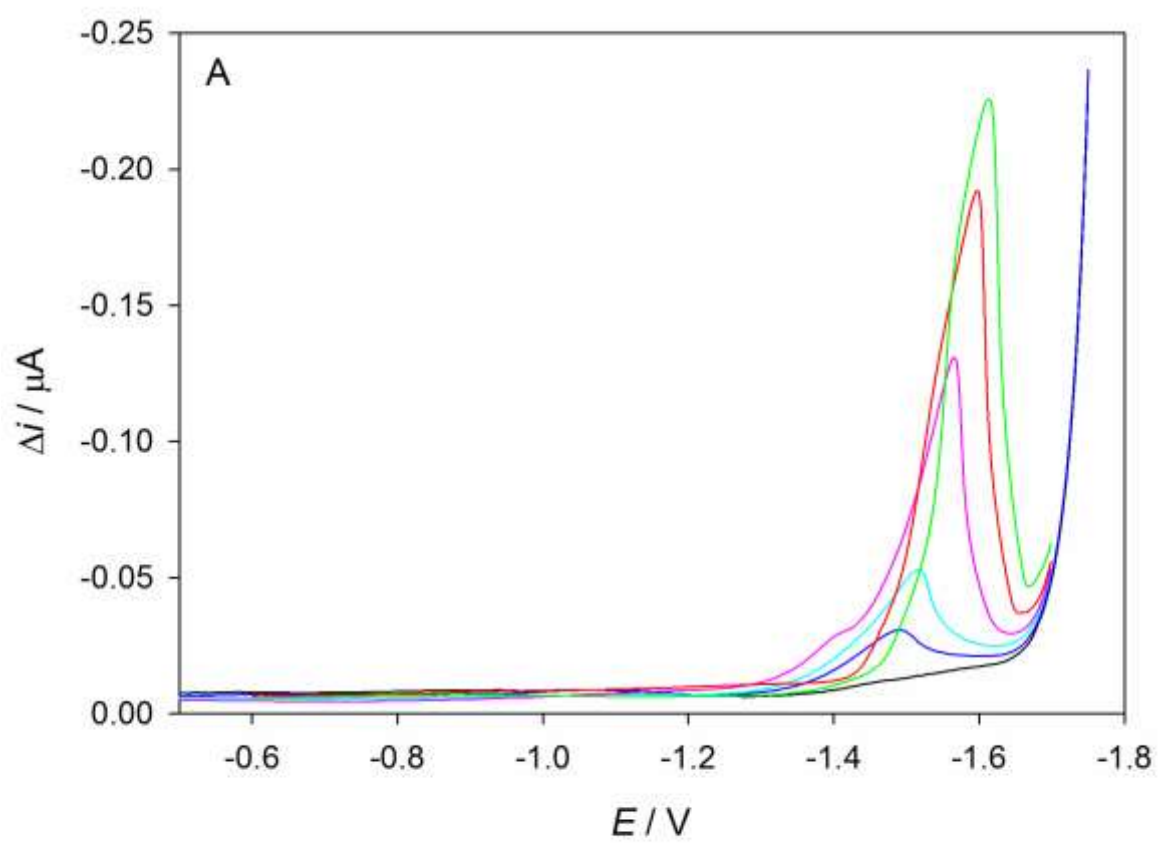


Figure 2A

1

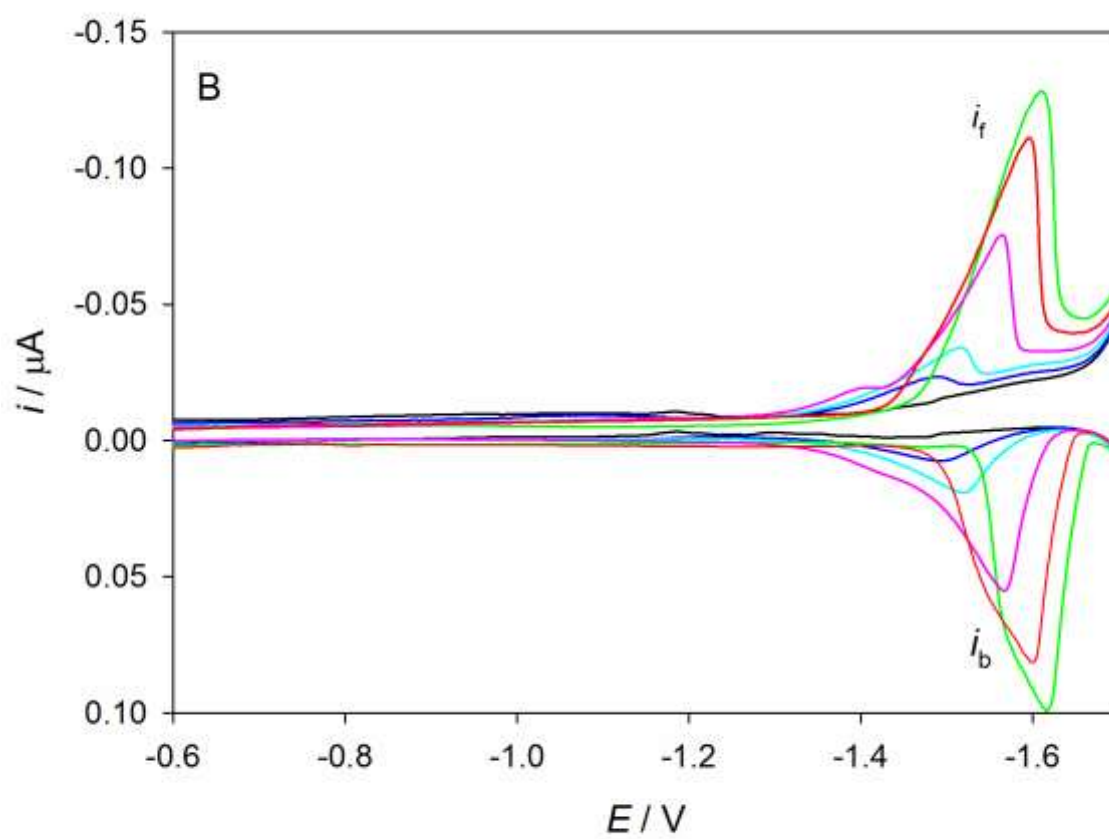


Figure 2B

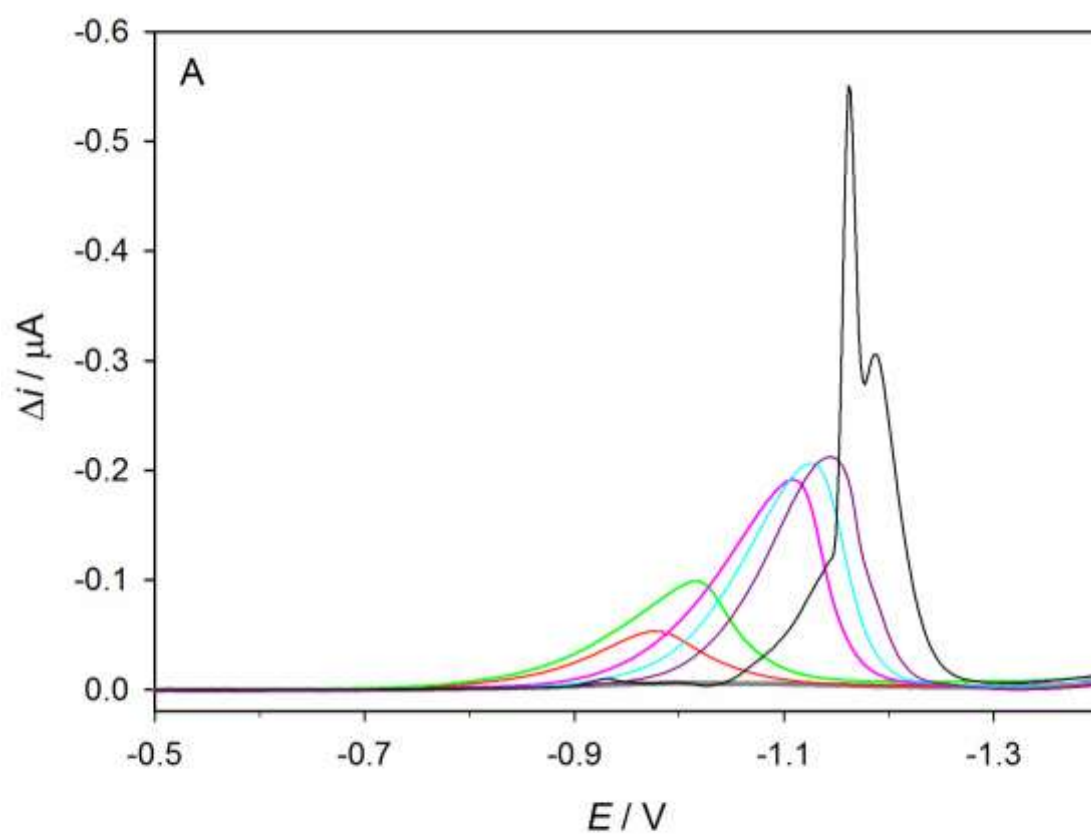


Figure 3A

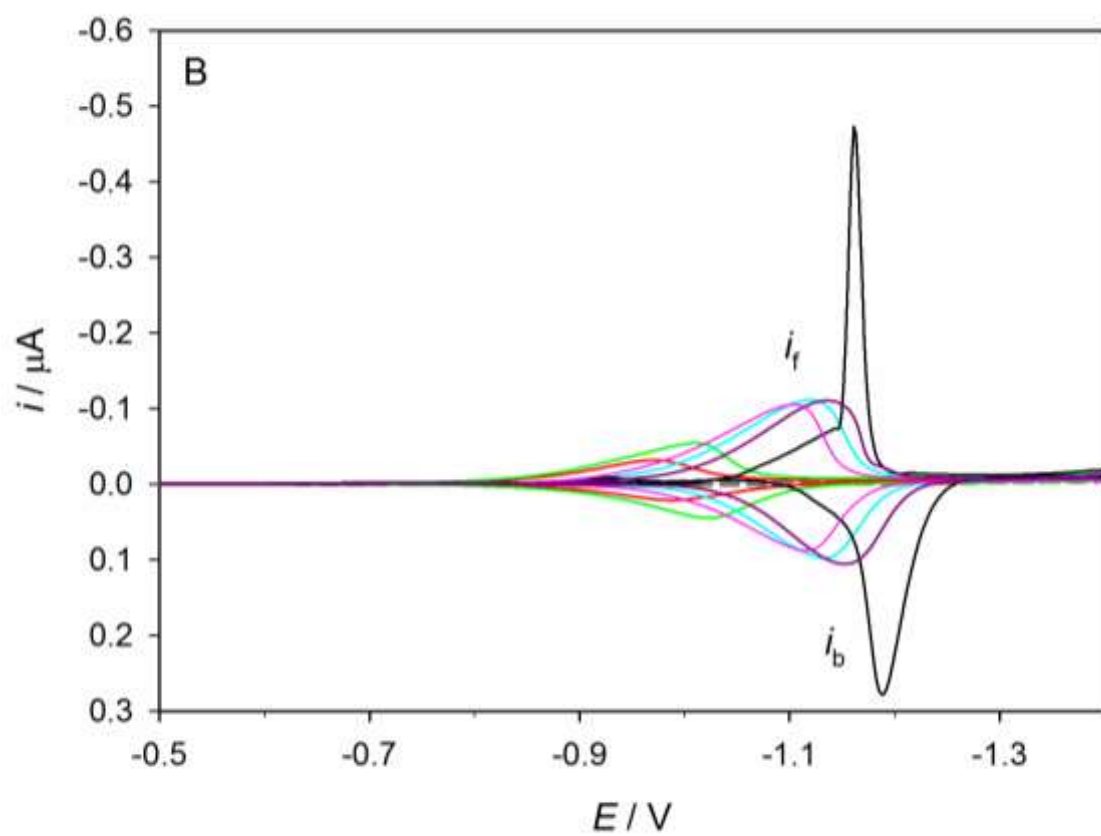


Figure 3B

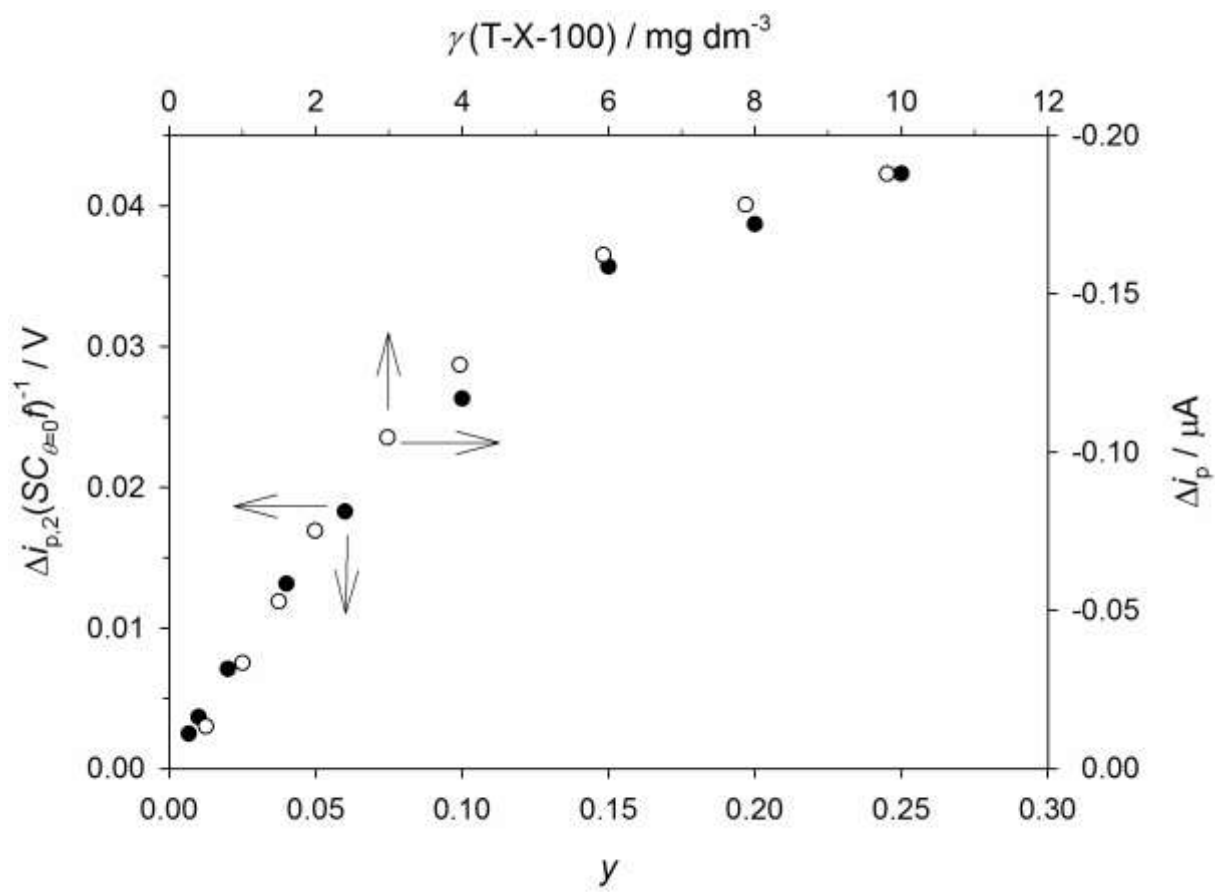


Figure 4

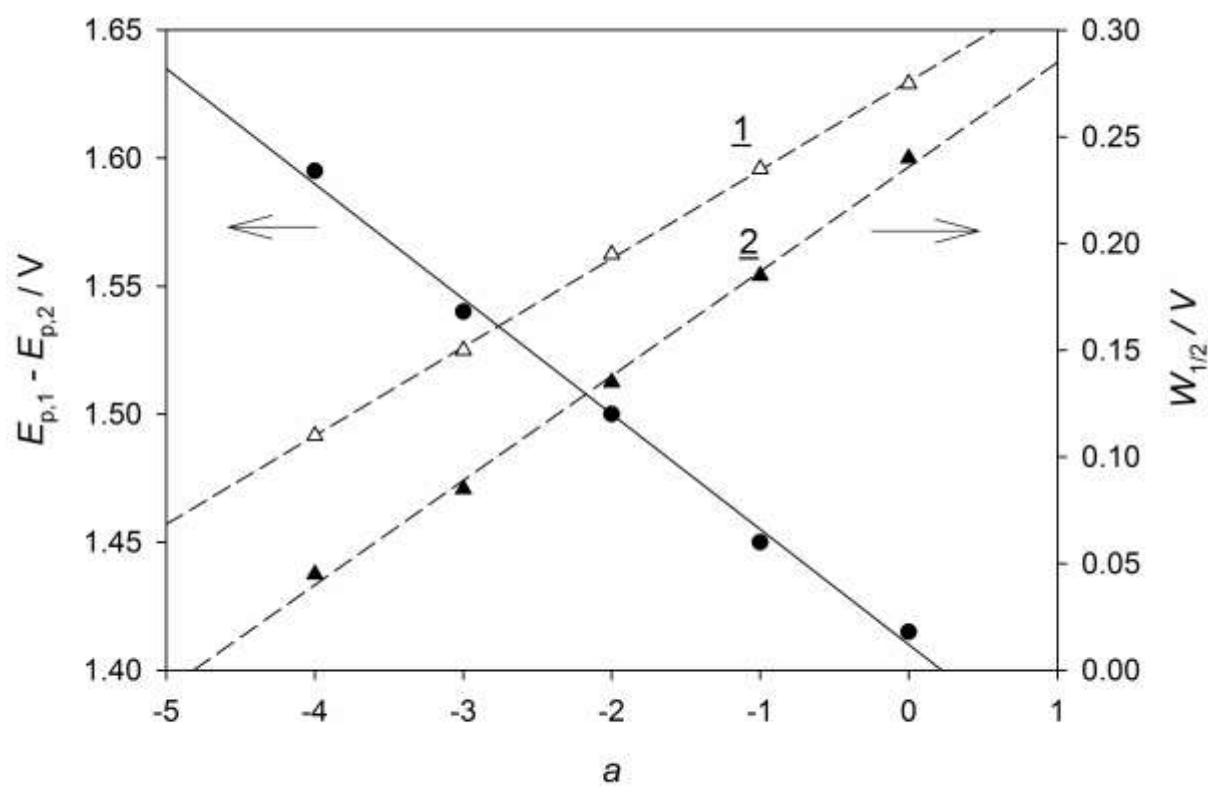


Figure 5

1

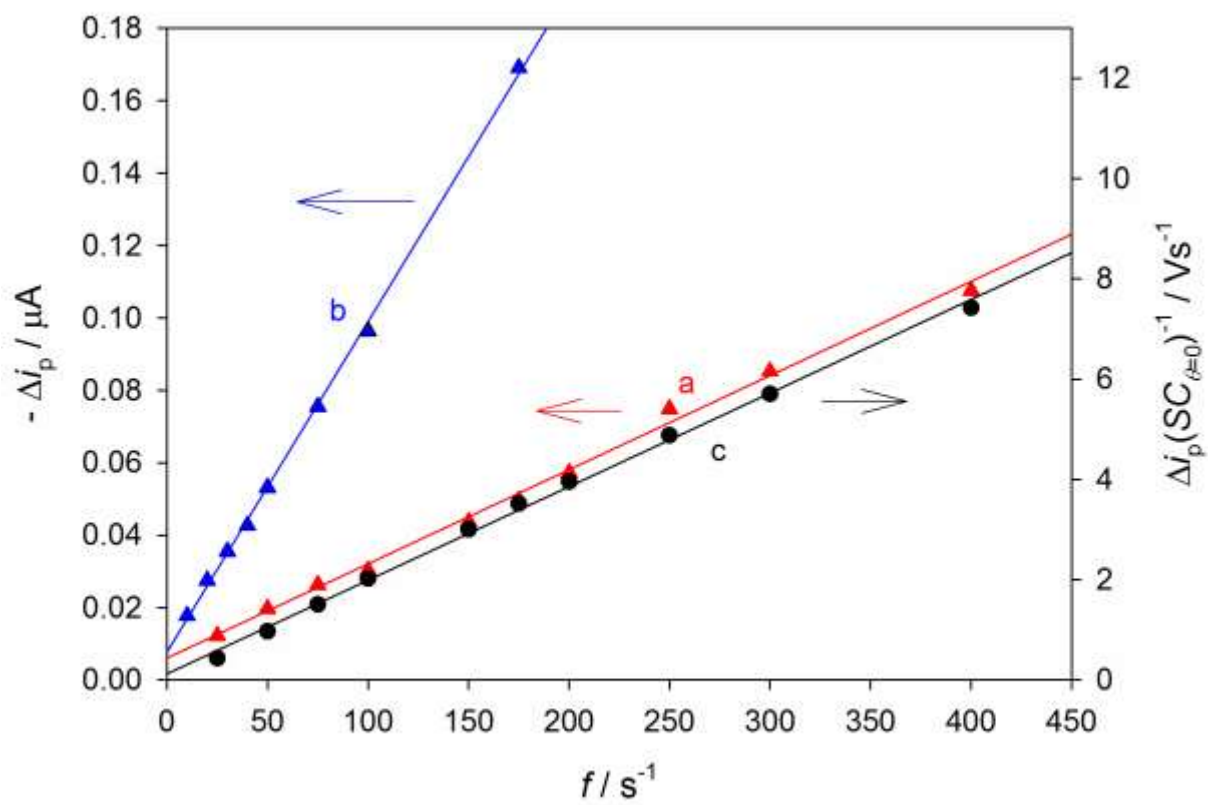


Figure 6

1

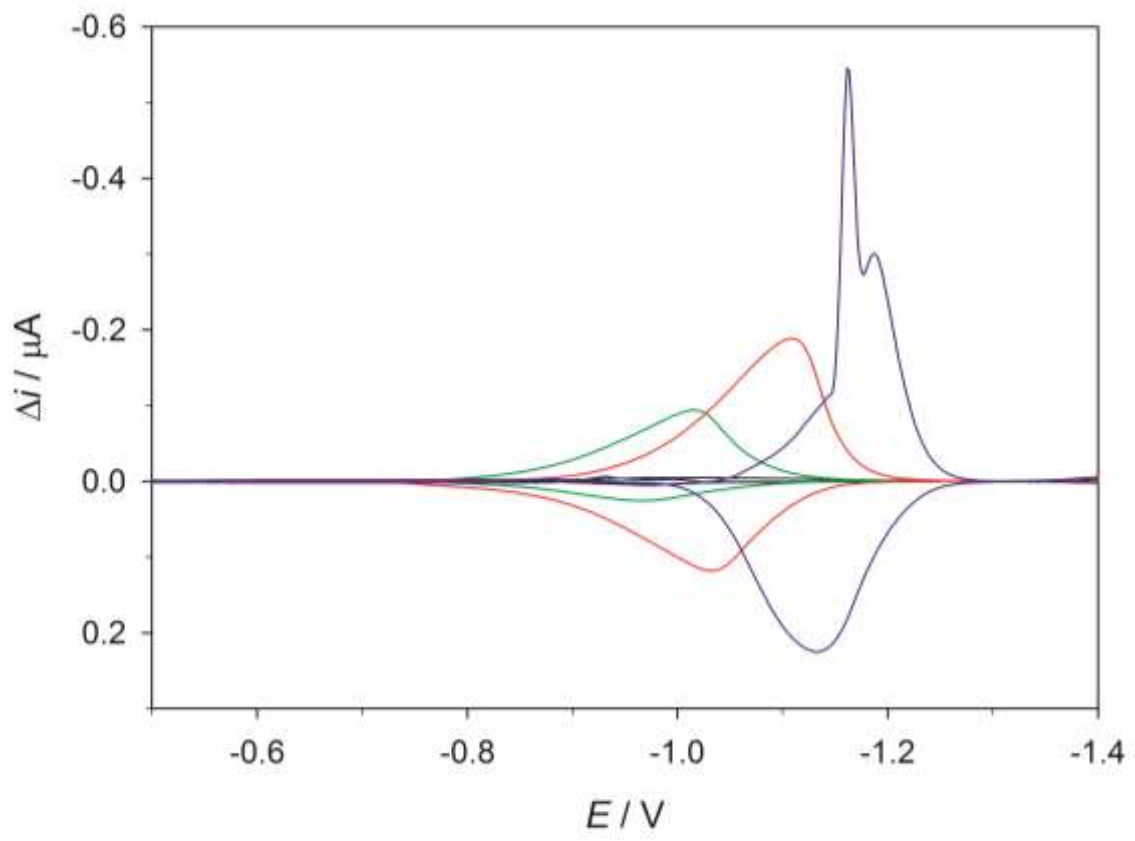


Figure 7